Segregation and Phase Transition in Mixed Lipid Films

Giulio Caracciolo,*,† Stefano Piotto,*,‡ Cecilia Bombelli,§,# Ruggero Caminiti,† and Giovanna Mancini§,#

Dipartimento di Chimica, Università degli Studi di Roma "La Sapienza", P.le A. Moro 5, 00185 Rome, Italy, Dipartimento di Ingegneria Chimica ed Alimentare, Università degli Studi di Salerno, Via Ponte Don Melillo, 84084 Fisciano, Salerno, CNR, IMC−Sezione Meccanismi di Reazione and Dipartimento di Chimica, Università degli Studi di Roma "La Sapienza", P.le A. Moro 5, 00185 Rome, Italy, and Centro di Eccellenza Materiali Innovativi Nanostrutturati per Applicazioni Chimiche, Fisiche e Biomediche

Received April 11, 2005. In Final Form: July 4, 2005

Energy dispersion X-ray diffraction (EDXD) was applied to investigate the structure of partly dehydrated mixed films formed by the phospholipid dimyristoyl phosphatidylcoline (DMPC) and any of the three diastereomers of the dicationic gemini surfactant (2S,3S)-2,3-dimethoxy-1,4-bis(*N*-hexadecyl-*N*,*N*-dimethylammonium) butane dibromide. As the surfactant to lipid molar ratio ($R_{S/L}$) increases, the gemini monotonically solubilizes the lipid bilayer promoting the formation of a cubic phase of space group $Pm\bar{3}n$ segregating from the residual lamellar phase of the lipid. Finally, at $R_{S/L} = 1$, the phase transition is complete. The mixed film at the highest surfactant to lipid molar ratio ($R_{S/L} = 2.3$) was hydrated by a vapor saturated atmosphere. At full hydration, a cubic to lamellar phase transition occurs. Coarse grain dynamic investigations, carried out as a function of both the surfactant to lipid molar ratio and the number of water molecules for amphiphile unit, allowed us to elucidate the structure of the emerging cubic phase and the hydration-induced structural pathway of the cubic to lamellar phase transition observed by EDXD.

Introduction

Surfactant/lipid mixed systems are currently used as model systems for elucidating the mechanism and compositionally driven pathway of the nonlamellar phase development in lipid membranes.[1−6] It is known that the formation of specific regions, featuring composition and physical properties different from the average properties of the bio-membrane, is crucial for the membrane itself to perform many important functions; however, an adequate description of their morphology and dynamics has not been given yet.

The study of aggregates on solid surfaces has some advantages with respect to the investigation of aqueous aggregate suspensions, such as the availability of several tools of investigation and a high sensitivity. Direct and indirect methods are, in fact, usually used to investigate aggregates on solid surfaces, and these include imaging atomic force microscopy (AFM), attenuated total reflection Fourier transform IR spectroscopy (ATR-FTIR), scanning electron microscopy, X-ray photoelectron spectroscopy (XPS), and neutron reflection.[7,8]

Here we report an investigation on surface aggregates formed by dimyristoyl phosphatidylcoline (DMPC) and any of the three diastereomers of gemini surfactants **1**, i.e., (2*S*,3*S*)-2,3-dimethoxy-1,4-bis(*N*-hexadecyl-*N*,*N*-dimethylammonium)butane di bromide, **1a**, (2*R*,3*R*)-2,3-dimethoxy-1,4-bis(*N*-hexadecyl-*N*,*N*-dimethylammonium)butane di bromide, **1b** and, (2*S*,3*R*)-2,3-dimethoxy-1,4-bis(*N*-hexadecyl-*N*,*N*-dimethylammonium)butane di bromide, **1c** (Chart 1).

Gemini surfactants are a class of amphiphilic molecules whose scientific interest is due to the peculiar features derived from their molecular structure.[9,10] Geminis consist of two surfactant units joined by a spacer that increases the hydrophobicity of the dimeric surfactant with respect to that of the monomeric units. As a result, the critic micellar concentration (cmc) of geminis can be up to 100 times lower than that of the corresponding monomeric surfactants. Although the aggregation properties of geminis in solution have been extensively studied over the past decades, their adsorption at interfaces both as single components and in mixed systems has received little attention so far. The morphology of gemini surfactants adsorbed at the silica−aqueous interface has been recently investigated as a function of the spacer group length.[11] Although the effect of spacer stereochemistry has been studied for anionic geminis,[12] as far as we know, no structural study has been devoted to the role of the spacer

* To whom correspondence should be addressed. E-mail: g.caracciolo@caspur.it (G.C.); piotto@unisa.it (S.P.). Tel: 0039 06 49913661. Fax: 0039 06 490631.

† Dipartimento di Chimica, Università degli Studi di Roma "La Sapienza".

‡ Università degli Studi di Salerno.

§ IMC−Sezione Meccanismi di Reazione and Dipartimento di Chimica, Università degli Studi di Roma "La Sapienza".

Centro di Eccellenza Materiali Innovativi Nanostrutturati per Applicazioni Chimiche, Fisiche e Biomediche.

(1) Koynova, R.; Tenchov, B. *Curr. Opin. Colloid Interface Sci.* **2001**, *6*, 277.

(2) Almgren, M. *Biochim. Biophys. Acta* **2000**, *1508*, 146.

(3) Funari, S. S.; Rapp, G. *Proc. Natl. Acad. Sci. U.S.A.* **1999**, *96*, 7756.

(4) Lichtenberg, D.; Opatowsky, E.; Kozlov, M. M. *Biochim. Biophys. Acta* **2000**, *1508*, 1.

(5) le Marie, M.; Champeil, P.; Møller, J. V. *Biochim. Biophys. Acta* **2000**, *1508*, 86.

(6) Maxifield, F. R. *Curr. Opin. Cell Biol.* **2002**, *14*, 483.

(7) Ducker, W. A.; Wanless, E. J. *Langmuir* **1996**, *12*, 5915.

(8) Blom, A.; Duval, F. P.; Kovacs, L.; Warr, G. G. *Langmuir* **2004**, *20*, 1291.

(9) Menger, F. M.; Keiper, J. S. *Angew. Chem. Int. Ed.* **2000**, *39*, 1906 (and references therein).

(10) Perez, L.; Torres, J. L.; Manrese, A.; Solans, C.; Infante, M. R. *Langmuir* **1996**, *12*, 5296.

(11) Atkin, R.; Craig, V. S. J.; Wanless, E. J.; Biggs, S. *Adv. Colloid Interface Sci.* **2003**, *103*, 219.

(12) Sommerdijk, N. A. J. M.; Hoeks, T. H. L.; Synak, M.; Feiters, M. C.; Nolte, R. J. M.; Zwanenburg, B. *J. Am. Chem. Soc.* **1997**, *119*, 4338.

10.1021/la050958d CCC: $30.25
Published on Web 08/27/2005

Chart 1. Chemical Structure of the Gemini Surfactants 1 (1a, 1b, 1c, from the Left to the Right)

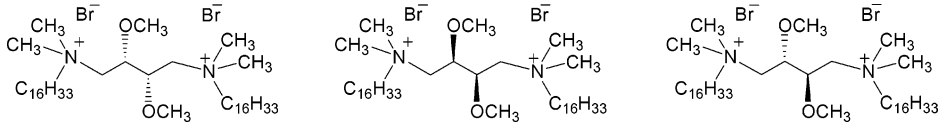

stereochemistry on the morphology of cationic surfactant/lipid systems at the solid/air interface.

The morphology of **1a**/DMPC, **1b**/DMPC, and **1c**/DMPC mixtures at the solid/air interface was investigated as a function of the surfactant/lipid molar ratio by energy dispersive X-ray diffraction (EDXD). Moreover a coarse grain dynamic investigation of the systems aimed at clarifying the evidences obtained by EDXD was carried out.

The effect of the presence of **1a** in DMPC liposomes had been investigated in solution in the context of the characterization of new cationic lipid based formulations to be used as photosensitizer delivery systems in photodynamic therapy.[13]

Experimental Section

Samples Preparation. Samples of **1** were prepared as elsewhere described.[13] The aqueous dispersions of the **1**/DMPC samples were prepared according to the procedure described by Hope et al.[14] A film of lipid (total 20.0 μmoles) was prepared on the inside wall of a round-bottom flask by evaporation of $CHCl_3$ solutions containing the proper amount of **1** and DMPC. The obtained films were stored in a desiccator overnight under reduced pressure and were then added to 1 mL of PBS buffer solution (10^{-2} M pH 7.4). The solution was vortex-mixed and then freeze−thawed six times from liquid nitrogen to 313 K. Extruded vesicles were prepared passing the dispersions 10 times through a 100 nm polycarbonate membrane (Whatman Nucleopore). The extrusions were carried out at 307 K, well above the transition temperature of DMPC (297.2 K), using a 2.5 mL extruder (Lipex Biomembranes, Vancouver, Canada). The mixtures were prepared at six different surfactant-to-lipid molar ratios $R_{S/L} = 0.25$, 0.43, 0.67, 1, 1.5, and 2.3. Mixtures above the 0.67 ratio were not extruded, because they yield a gel. All of the aqueous dispersions were deposited onto the freshly cleaved ⟨100⟩ surface of oriented silicon wafers, and the solvent was allowed to evaporate under a gentle nitrogen flux. The temperature of the sample was fixed at 300 K. Dehydrated films were characterized at the equilibrium with the surrounding environment (relative humidity, RH ∼ 50%). Last the film at the highest $R_{S/L}$ was fully hydrated from the vapor and characterized by means of EDXD.

EDXD Experiments. The diffraction experiments were carried out at the powder diffraction laboratory (Dipartimento di Chimica), using an energy dispersive X-ray diffractometer elsewhere described.[15,16] The diffracted intensity is a function of the exchanged momentum $q = cE \sin\theta$ ($c = 1.014$ Å^{-1} keV^{-1}) so that we can perform our measurements at a fixed diffraction angle using a polychromatic Bremmstrahlung radiation (11−50 keV region), produced by a standard Seifert tube and a solid-state EG&G detector. The minimum angle increment and reproduction is 0.005°. As a result of intrinsic differences with traditional angular dispersive apparatuses, by increasing the diffraction angle higher q values can be scanned. Reflection-mode EDXD patterns from **1**/DMPC assemblies depositated on the ⟨100⟩ surface of silicon wafers were recorded at two diffraction angles $\theta = 0.35°$ and 0.75° covering an overall q-range between 0.081 and 0.730 Å^{-1}. The various portions of the diffraction spectrum are routinely united utilizing the overlap of adjacent zone in order to obtain a unique q curve.[15,16] Anyway, since the aim of this work was the investigation of the morphological features of **1** and **1**/DMPC surface aggregates rather than a quantitative analysis of these structures, here we report the rough EDXD curves disjointedly. Typical acquisition times, depending on the sample concentration and the desired accuracy of experimental data, varied between 1000 and 100 000 s. Such exposure times do not damage biological samples as elsewhere discussed.[17] EDXD data were normalized to the intensity of the incident beam. Parasitic effects arising from collimations slits and the silicon substrates were suitably corrected.

Theoretical Calculations. *Dissipative Particle Dynamics Investigation.* A dissipative particle dynamics (DPD) approach was used; this is a powerful, off-lattice, dynamical model. In a DPD simulation, a particle represents the center of mass of a cluster of atoms. The total force on such a particle consists of dissipative, random, and conservative forces. The dissipative and random forces are chosen such that a proper canonical distribution is sampled.[18,19]

In the lipid-water−surfactant model, three types of particles, w, h, and t, were used to mimic water and the head and tail atoms of a lipid, respectively. The hydrophilic and hydrophobic particles interact via a soft-repulsion model commonly used in DPD,[18,19] and their mutual interactions are expressed in terms of repulsion parameters. The DPD parameters are related to the compressibility of water and to Flory−Huggins solubility parameters such that a reasonable description of the thermodynamics of the real system can be obtained.[18] We considered DMPC consisting of a headgroup with three hydrophilic segments and two tails with a length of 4 units. The headgroup is parametrized to include the presence of bromide counterions[18,19] We assumed that a DPD particle has a volume of 90 Å^3, using the phospholipid component volumes determined by Armen et al.[20] The gemini surfactant consists of three hydrophilic beads and two tails at the ending with a length of 5 units (t5h3t5).

It is essential, for a correct description of the experimental chain length dependence of the area per lipid, to properly reproduce the conformations of the lipid. Molecular dynamics simulations of a single phospholipid in water using a realistic all-atom representation were used to generate configurations of the lipid, which were subsequently used to optimize the intramolecular interactions (bond-bending and bond-vibration) of the DPD model.[21] This method led to values conforming to the ones used by Groot and Warren[18] for the soft-repulsions in the conservative DPD interactions ($a_{ww} = a_{tt} = 25$, $a_{ht} = a_{wt} = 80$, $a_{hh} = 35$, and $a_{hw} = 15$). Diastereomeric interactions and different counterions[18,19] can be taken into consideration by varying the terms a_{hh} and a_{hw}. The simulations were carried out at 295 K in water solution for lengths from 200 and 400 ns using the software DPD from Accelrys.[22] The water content ranged from 2 to 24 water molecule per lipid molecule. The simulation box was of 134 × 107 × 107 Å.

Topological Approach. A powerful topological strategy was worked out with the help of periodic nodal surfaces (PNS), as they are defined by von Schnering & Nesper,[23] for generating an envelope of surfaces in real space. This approach utilizes a Fourier Ansatz, which codes the fundamental topological information of a space group or of a specific structure in the form of a short

(13) Bombelli, C.; Caracciolo, G.; Di Profio, P.; Diociaiuti, M.; Luciani, P.; Mancini, G.; Mazzuca, C.; Marra, M.; Molinari, A.; Monti, D.; Toccaceli, L.; Venanzi, M. *J. Med. Chem.* (in press).

(14) Hope, M. J.; Bally, M. B.; Webb, G.; Cullis, P. R. *Biochim. Biophys. Acta* **1985**, *812*, 55.

(15) Caminiti, R.; Rossi Albertini, V. *Int. Rev. Phys. Chem.* **1999**, *18* (2), 263.

(16) Rossi Albertini, V.; Appetecchi, G. B.; Caminiti, R.; Croce, F.; Cilloco, F.; Sadun, C. *J. Macromol. Sci. Phys. B* **1997**, *36* (5), 629.

(17) Caracciolo, G.; Sadun, C.; Caminiti, R.; Pisani, M.; Bruni, P.; Francescangeli, O. *Chem. Phys. Lett.* **2004**, *397*, 138.

(18) Groot, R. D.; Warren, P. B. *J. Chem. Phys.* **1997**, *107*, 4423.

(19) Frenkel, D.; Smit, B. *Understanding molecular simulations: from algorithms to applications*; Academic Press: London, 2002.

(20) Armen, R. S.; Uitto, O. D.; Feller, S. E. *Biophys. J.* **1998**, *75*, 734.

(21) Kranenburg, M.; Laforge, C.; Smit, B. *Phys. Chem. Chem. Phys.* **2004**, *6*, 4142.

(22) Accelrys, http://www.accelrys.com.

(23) von Schnering, H. G.; Nesper, R. *Z. Phys. B*, *Condensed Matter* **1991**, *83*, 407.

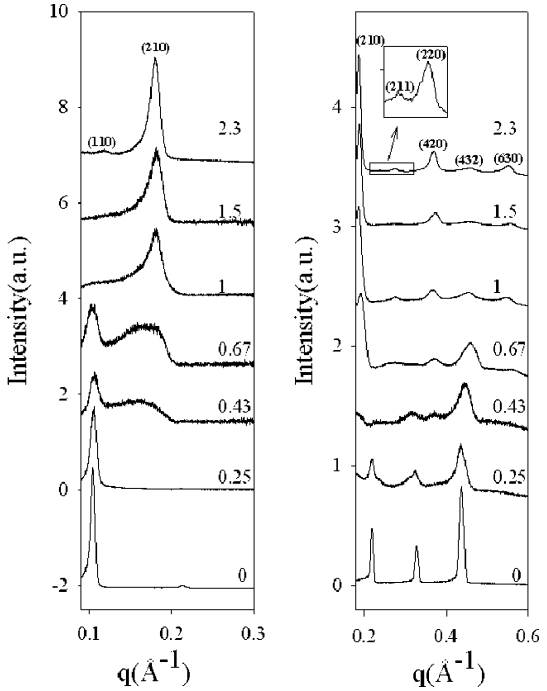

Figure 1. EDXD patterns of **1a**/DMPC mixtures collected at $\theta = 0.35°$ (left panel) and $\theta = 0.75°$ (right panel) as a function of increasing surfactant to lipid molar ratio (from the bottom to the top). Lipid bilayer structure of pure DMPC is gradually destroyed by the addition of **1a**: at $R_{S/L} = 0.43$ a new phase emerges which segregates from the lamellar phase of residual DMPC up to $R_{S/L} = 0.67$, whereas at $R_{S/L} = 1$, a complete transition occurs. At $R_{S/L} = 2.33$, a cubic phase of space group $Pm\bar{3}n$ can be detected.

Fourier summation. A family of surfaces in real space can be generated from a Fourier summation according to the expressions

$$f(xyz) = \sum_{hkl} S(Hkl) \cos(2\pi(hx + ky + lz) - \alpha(hkl))$$

where $S(hkl)$ is the structure factor, hkl indicate the reflex, and α is the phase.

The surfaces are periodic equi-surfaces (PES).[23] PES represent the topological characteristics of either a space group or a structure (type) or set of structures. Although an arbitrary number of Fourier coefficients may be chosen, only summations with a small number of structure factors were proven to be useful for the elucidation of the general topological features of a structure or a set of structures of a given symmetry.[23] The envelope functions are very useful descriptors of atomic, group displacements, or clusters of molecules, or conformational changes involved in a phase transition. They reflect the deformation of a network by the change of the connectedness of the labyrinths measured by the variation of the genus.

Results

EDXD Results. EDXD patterns of mixed **1a**/DMPC and **1c**/DMPC films on silicon wafers are reported in Figures 1 and 2, respectively, where they are both compared with the X-ray pattern of pure DMPC ($R_{S/L} = 0$) showing the first four Bragg reflections (*00l*) of an ordered multilamellar structure. The patterns obtained by **1b**/DMPC films are identical to those relative to **1a**/DMPC mixtures (data not reported).

Figure 3 shows the EDXD patterns of solid-supported geminis **1a**, **1b**, and **1c**.[24] As evident, the geminis self-assemblies at the solid/air interface are extremely ordered

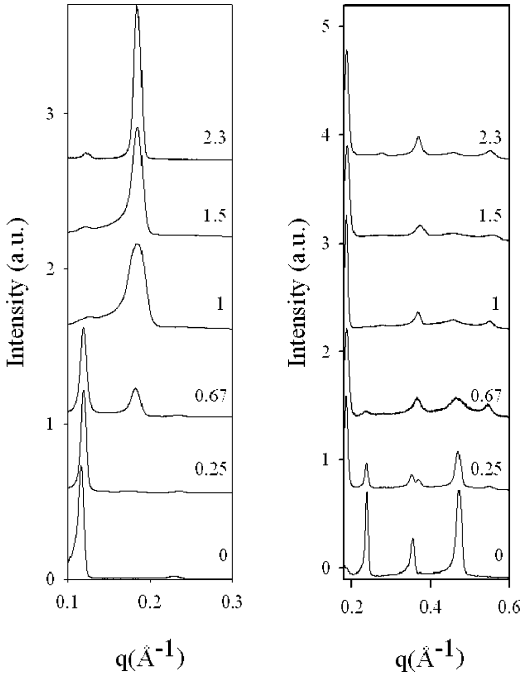

Figure 2. EDXD patterns of **1c**/DMPC mixtures at $\theta = 0.35°$ (left panel) and $\theta = 0.75°$ (right panel).

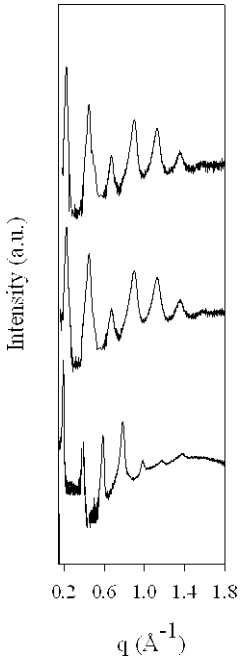

Figure 3. EDXD patterns of dried **1a**, **1b**, and **1c** (from the top to the bottom) samples at the solid/air interface. The surface aggregates are very ordered multibilayers.

Table 1. Packing Symmetry of Solid-Supported Gemini Surfactants at the Solid/Air Interface

sample	packing simmetry	d_{ob}(Å)
1a	bilayers	28.4
1b	bilayers	28.4
1c	bilayers	31.9

multilamellar structures. For the sake of clarity, we report in Table 1 the packing symmetry and the repeat distances of gemini **1** samples obtained by experiments carried out in dried conditions. X-ray diffraction patterns of **1**/DMPC mixture at surfactant-to-lipid molar ratio between $R_{S/L} = 0.25$ and $R_{S/L} = 1$ show that the intensity and sharpness of all the Bragg maxima due to the lamellar structure

(24) Caracciolo, G.; Mancini, G.; Bombelli, C.; Luciani, P.; Caminiti, R. *J. Phys. Chem. B* **2003**, *107*, 12268.

Table 2. X-ray Diffraction Data for the 1/DMPC Sample (RS/L=2.3) Indexed to the Space Group $Pm\bar{3}n$

hkl	$h^2 + k^2 + l^2$	d_{obs} (Å)	d_{cal} (Å)
110	2	54.6	54.6
200	4	39.0	38.6
210	5	34.5	34.5
211	6	31.3	31.5
220	8	27.3	27.6
310	10	24.3	24.4
420	20	17.3	17.3
432/520	29	14.4	14.3
630	45	11.5	11.5

of DMPC monotonically decrease as a function of increasing $R_{S/L}$.

The diffraction pattern of the mixture at $R_{S/L} = 0.25$ (Figures 1 and 2, left panel) shows the presence of the lamellar phase of pure DMPC. At $R_{S/L} = 0.43$, the EDXD pattern, resembling that of DMPC, actually arises from two distinct phases. By comparing the diffraction patterns collected at $\theta = 0.75°$ (Figures 1 and 2, right panel, $R_{S/L} = 0.67$) with that of bare lipid we observe that the lamellar structure of DMPC is strongly perturbed by the addition of surfactant.

On the other hand, diffraction data do not permit a plain interpretation of this emerging contribution whose position in the q space is not in anyway related to that of **1a** and **1c** surface aggregates (Figure 3). At increased surfactant, remarkable changes in the system are produced, and it unmistakably starts to present a proper behavior. In fact, even if the first-order Bragg peak of residual DMPC is present up to $R_{S/L} = 0.67$ the growing phase becomes more evident. At $R_{S/L} = 1$, the lamellar structure of DMPC is no more detectable and a single phase exists, its diffraction peaks being sharp and dominant. Analogous consideration can be made on the EDXD patterns recorded at $R_{S/L} = 1.5$. Finally, at $R_{S/L} = 2.3$ the EDXD patterns collected at $\theta = 0.35°$ and 0.75° unambiguously show the presence of a cubic phase with reflections at distinct ratios. They were indexed as (110), (200), (210), (211), (220), (310), (420), (432)/(520), and (630) reflections of a cubic phase of space group $Pm\bar{3}n$ as reported in Table 2.

Our experimental resolution (~0.002) Å^{-1} ensures that the diffraction peak centered at $q \sim 0.115$ Å^{-1} is not the (*001*) crystallographic reflection of pure multilamellar DMPC ($q \sim 0.107$ Å^{-1}). In the raw EDXD pattern of Figure 4, the (200) reflection is not evident, but a complete deconvolution of the spectrum definitely allows us to recognize it. This indexation gives establishment of the cell parameter $a = (2\pi/q_{110})(2)^{0.5} = 77.3$ Å. Interestingly, it must be pointed out that the emerging structure is completely different from those of the geminis and of the lipid alone, and it is really the result of interactions characteristic of the binary mixture. The dried film with the highest percentage of surfactant ($R_{S/L} = 2.3$), which do not show any residual trace of the DMPC bilayer structure, was finally hydrated by vapor until traces of water condensation onto the film were detected. At this point, the system was in the biologically relevant excess water condition. The hydration process induced a phase transition from the cubic phase to a new lamellar structure as shown by the EDXD patterns of Figure 5.

The high background intensity due to hydration molecules does not hinder the new phase reflections and the second, third, and fourth orders are clearly distinguishable (Figure 5, right panel). The varying background in the EDXD pattern is due to the scattering of excess water condensed at the lipid/air interface. The emerging structure has a lamellar periodicity $d = 45.6$ Å intermediated

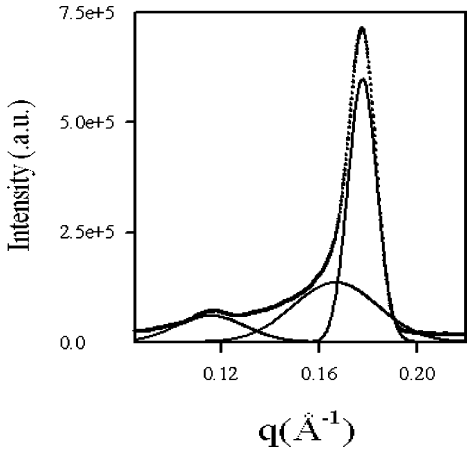

Figure 4. Overall EDXD pattern of **1a**/DMPC ($R_{S/L} = 2.3$) collected at $\theta = 0.35°$ arises from the superposition of three distinct distributions centered at $q = 0.115$, 0.161, and 0.182 Å^{-1} which are indexed as the (110), (200), and (210) reflections of a cubic phase of space group $Pm\bar{3}n$ (Q^{223}).

between those of fully hydrated DMPC ($d = 63.3$ Å) and **1a** ($d = 28.7$ Å). Due to intrinsic fluctuations in hydrated fluid bilayers, X-ray data from multilamellar arrays can only yield electron density profiles (EDPs) along the normal to the bilayers giving a measure of the bilayer thickness d_{HH} and the size of the water region d_W. From the EDXD patterns of Figure 5, the EDP along the normal to the bilayers was calculated (not reported) as elsewhere described.[17] It provided an estimation of both the bilayer thickness ($d_{HH} = 30.7$ Å) and the thickness of the water region ($d_W = 14.9$ Å) of the hydration-induced lamellar phase.

Computational Analysis Results. To elucidate the inner structure of the aggregate at $R_{S/L} = 2.3$, we employed the surface topological strategy described above. The structure depicted in Figure 6 appears by using the first 3 reflections of the EDXD pattern ((110), (210), and (211) with $\alpha = 0$) permuted in the space group $Pm\bar{3}n$. These small sets of structure factors are not arbitrarily chosen, in fact, only those (*hkl*) combinations are considered that arise when systematically starting off from the center of reciprocal space. The envelopes represent rod packing of elongated micelles accordingly with the structure previously indicated by Hyde.[25] The visualization of the Gaussian curvature color mapped onto the surfaces, reflects the micellar origin of the aggregate. The calculation of the surfaces and the Gaussian curvature have been performed with the program CURVIS.[26] A coarse grain dynamics investigation was carried out varying lipid composition (with particular attention to the system at $R_{S/L} = 2.3$) and water content, precisely 24, 17, 12, 7, and 2 water molecules per amphiphilic molecule.

By definition coarse grain simulations are not extremely accurate for systems with a strong asymmetry in compositions (such the case of 2 water molecules). Nevertheless, the DPD simulations give indication about the most thermodynamically stable aggregate, and, additionally, highlight the morphological changes caused by different composition. In this simulation diastereomeric interactions were not taken into consideration through the variation of terms a_{hh} and a_{hw}, though at high percentages of gemini they could be in principle important, because the diffraction patterns relative to the three diastereomers do not show relevant differences.

(25) Hyde, S. in Handbook of Applied Surface and Colloid Chemistry; Holmberg, K., Ed.; John Wiley & Sons: New York, 2002; Vol. 2.
(26) Piotto, S. P.; Nesper, R. *J. Appl. Cryst.* **2005**, *38*, 223.

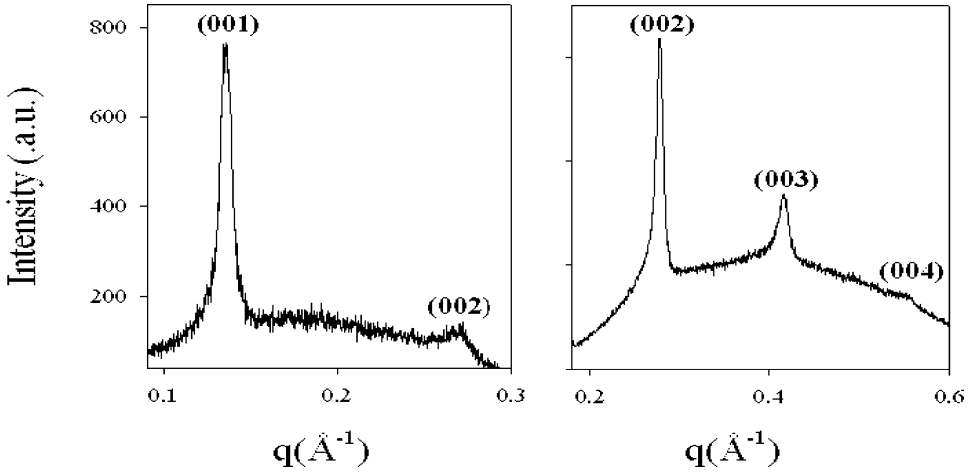

Figure 5. EDXD patterns of fully hydrated 1a/DMPC sample ($R_{S/L} = 2.3$) at $\theta = 0.35°$ (left panel) and $\theta = 0.75°$ (right panel). The first four (*00l*) reflections of a lamellar phase are detected.

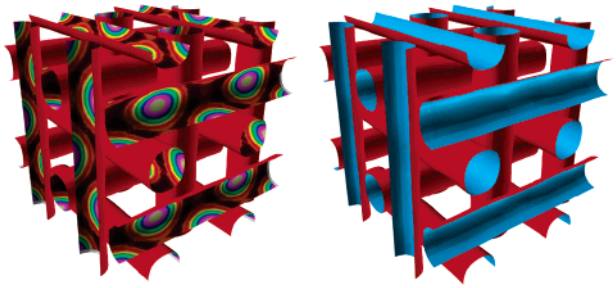

Figure 6. Packing of elongated micelles in the spacegroup *Pm*3*n*. The Gaussian curvature is mapped onto one side of the surface to evidence the micellar origin of the structure.

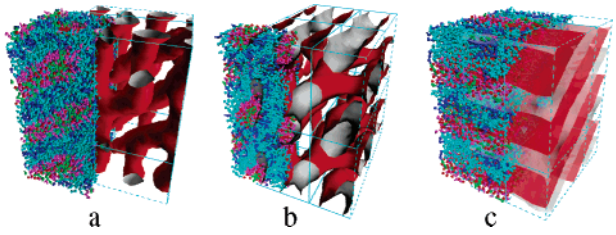

Figure 7. Spatial organization of DMPC-gemini-water system ($R_{S/L} = 2.3$) at concentration of 2 (a), 7 (b), and 12 (c) water molecules per amphiphile unit. On the left of each picture the molecules are represented as balls and sticks. The colors are as follows: water, red; head DMPC, green; tail DMPC, dark blue; head **1**, fuchsia; tail **1**, light blue. On the right of the picture, the surfaces separating the water space from the lipid space permit to capture the topological organization of the aggregate.

The results of the simulation concerning the mixtures with high percentage of DMPC ($R_{S/L}$ in the range 0.25−1.5) are in full agreement with those of EDXD experiments (data not reported). At $R_{S/L} = 2.3$ and at low water content (2 water molecules per unit of amphiphile), DMPC and gemini surfactant spontaneously organize into rod structures with a diameter of about 30 Å as shown in Figure 7a. Within the time limit of the computer simulation, a clear, highly symmetric organization is not evident, probably because the calculation did not converge. At higher water content (7 water molecules per unit of surfactant), the rods appear bicontinuous and interconnected (Figure 7b). In condition of full hydration (12 water molecules per unit of amphiphile) a lamellar phase appears (Figure 7c).

Packing symmetry and periodicities of the structure shown in Figure 7c are given in Table 4 where they are compared to the findings obtained by EDXD.

Table 3. Structural Parameters of the Full *q* Refinement Model [ref 28] Adapted from Reference 27

	DMPC	1a
d	63.3	28.7
d_{HH}	46.8	24.6
d_W	16.5	4.1
n_w	29	3.5

Table 4. Packing Symmetry and Periodicities of the DMPC/1 Mixed Film ($R_{S/L} = 2.3$, at Concentration of 12 Water Molecules Per Amphiphile Unit)

	EDXD	DPD
packing symmetry	bilayers	bilayers
d (Å)	45.6 ± 1	55 ± 5
d_{HH} (Å)	30.7	34 ± 5
d_W (Å)	14.9	21 ± 5

Discussion

We recently reported on the results of EDXD measurements carried out on solid-supported films of gemini **1**.[24] As reported in Table 1, the features of gemini **1a** and **1b** are, as expected, identical, whereas the lamellar periodicity of **1c** is about 3 Å larger than that obtained by **1a**(**b**), as also shown in Figure 3.

In a recent paper,[27] we also reported on the physical properties of both DMPC and **1a** surface aggregates and the X-ray data were analyzed using a recently proposed full *q* refinement model.[28] The derived structural parameters such as the lamellar *d* spacing, the bilayer thickness and the size of the water region interbilayer are listed in Table 3. The deep difference in the bilayer thickness between DMPC and **1a** was explained in terms of different molecular packing. Although the phospholipid membrane is in the liquid-crystalline L_α phase in which the acyl chains are melted and experience trans−gauche isomerizations, **1a** surface aggregates have interdigitated chains. The thermogravimetric measurements carried out on **1** samples[24,27] revealed the same amount of water content (3.5 molecules of water for surfactant molecule) and suggested that the different stereochemistry of the spacer governs the extension and packing of hydrophobic chains of the aggregate systems at the air/solid and water/air interface, as well as in the bulk,[29] as a consequence of the exposure of polar groups to water. The aggregates formed

(27) Caracciolo, G.; Mancini, G.; Bombelli, C.; Caminiti, R. *Chem. Phys. Lett.* **2004**, *386*, 76.
(28) Pabst, G.; Rappolt, M.; Amenitsch, H.; Laggner, P. *Phys. Rev. E* **2000**, *62*, 4000.
(29) Mancini, G. to be published.

by the diastereomeric surfactant in water show in fact different features (morphology, Krafft point).[29]

Interestingly, the diffraction patterns obtained by the **1**/DMPC mixtures show that enantiomers **1a** and **1b** produce the same effect on the lamellar phase of DMPC, and the meso form **1c** has a very similar effect. This result was unexpected not only in the comparison between **1a**(**b**) and **1c**, that feature different aggregation behavior, but also in the comparison between enantiomers **1a** and **1b**, being their interactions with DMPC diastereomeric.

The physicochemical characterization carried out by different means put in evidence a phase transition at a $R_{S/L} = 0.67$, in correspondence of which the biological evaluation showed a decrease in the delivery efficiency.[29]

The EDXD results described above show the emergence of a new phase at a $R_{S/L} = 0.43$ and a complete transition at $R_{S/L} = 1$. The new phase, coexistent with the lamellar phase of DMPC at $R_{S/L} = 0.43$, is formed by a certain ratio of the two components, DMPC and gemini, and consequently segregates from the lamellar phase of residual DMPC. This evidence demonstrates the specificity of interactions governing the segregation in lipid aggregates.

At $R_{S/L} = 2.3$ the EDXD patterns shows the presence of a cubic phase of space group $Pm\bar{3}n$. The encountered cubic phase, first reported by Balmbra for dodecyltrimethylammonium chloride,[30] was extensively studied and has been the subject of some debate.[31−35] After the cage-like model made of a three-dimensional network of rods and spheres initially proposed by Tardieu and Luzzati,[31] Vargas et al.[35] described this structure as consisting of two types of disjointed micelles in close agreement with previous nuclear magnetic resonance results. Charvolin and Sadoc, on the basis of X-ray measurements and freeze-fracture electron microscopy, proposed a system consisting of two spherical and six oblate micelles per unit cell arranged on a cubic lattice and separated by a continuous film of water.[36] More recently, an alternative rod packing has been proposed: micelles within the phase can fuse through hexagonal phases, giving the well-known "β-W" rod packing ($Pm\bar{3}n$).[37] This same organization was obtained (Figure 6) through the topological analysis illustrated before by using the first three reflections of the EDXD pattern.

The molecular dynamics analysis carried out to clarify the molecular arrangement found by EDXD shows that in the presence of a few water molecules (2−7) per unit of amphiphile, the morphology of the aggregate, as result from the DPD calculations, is an interwoven network of distorted rods. This finding is in pretty good agreement with the arrangement obtained by the topological approach and consequently with the X-ray indexation of space group $Pm\bar{3}n$.

At full hydration, a cubic to lamellar phase transition occurs and the conclusions of DPD calculations (Figure 7c) are in good agreement with the structural results obtained by EDXD (Table 4).

In particular, although the thickness of the bilayer membrane calculated from the X-ray data ($d_{HH} = 30.7$ Å) closely resembles that obtained from DPD simulations ($d_{HH} = 34$ Å), the thickness of the water region ($d_W = 14.9$ and 21 Å from EDXD and DPP calculations respectively) is slightly different. Nevertheless, the water molecules per surfactant unit considered in the DPD calculation only represent an average value between those joined to the headgroup of DMPC and **1** molecules, respectively.[24] An overestimation of the effective number of water molecules at full hydration could result in a larger water layer, i.e., in a larger lamellar d spacing.

The very thin bilayers of **1** (Table 3) impose a much lower lamellar periodicity on the mixtures with DMPC which itself has thicker, nonintercalated bilayers. The larger headgroup area of **1** could comport an increase of the area for the DMPC headgroups and, consequently, a fluidification of the tails and a reduction of the lamellar spacing d. Alternatively, the increase in the headgroup area may favor an interdigitated phase as recently reported by Ryhänen et al.[38] Interdigitation would induce a denser packing of the hydrophobic chains.

Conclusions

We have determined the compositionally driven phase transition of the lamellar phase of DMPC induced by **1** gemini surfactants. By indexing X-ray diffraction patterns at reduced levels of hydration (RH $\sim$ 50%), we have identified a cubic phase of space group $Pm\bar{3}n$ (Q^{223}) which segregates from the lamellar phase of DMPC up to a complete phase transition. The topological analysis performed by using the reflections of the X-ray pattern showed a cubic phase in agreement with the "β-W" rod packing recently proposed for the Q^{223} cubic phase. X-ray measurements showed that hydrating the cubic phase leads to a lamellar phase plus excess water. DPD simulations confirmed the structural findings of EDXD elucidating the existence of an intermediate bicontinuous arrangement of distorted and interconnected rods between the micellar and the lamellar phase.

LA050958D

(30) Balmbra, R.; Clunie, R.; Goodman, J. S. *Nature (London)* **1969**, *222*, 1159.
(31) Tardieu, A.; Luzzati, V. *Biochim. Biophys. Acta* **1970**, *219*, 11.
(32) Luzzati, V. *Curr. Opin. Struct. Biol.* **1997**, *7*, 661.
(33) Mariani, P.; Luzzati, V.; Delacroix, H. *J. Mol. Biol.* **1988**, *204*, 165.
(34) Sakya, P.; Seddon, J. M.; Templer, R. H.; Mirkin, R. J.; Tiddy, G. J. T. *Langmuir* **1997**, *13*, 3706.
(35) Vargas, R.; Mariani, P.; Gulik, A.; Luzzati, V. *J. Mol. Biol.* **1992**, *225*, 137.
(36) Charvolin, J.; Sadoc, J. F. *J. Phys. (Paris)* **1988**, *49*, 521.
(37) Hyde, S. T. *Handbook of Applied Surface and Colloid Chemistry*; Wiley: New York, 2001; Chapter 16.
(38) Ryhänen, S. J.; Alakoskela, J. M. I.; Kinnunen, P. K. J.; *Langmuir* **2005**, *21*, 5707 (and references therein).